Superficies y Vacío 1, 59-65(1989) © *Sociedad Mexicana de Ciencia de Superficies y de Vacío*

DIELECTRIC PROPERTIES AND GROWTH KINETICS OF (001) GaAs SURFACES DURING CRYSTAL GROWTH BY MBE AND OMCVD: REAL-TIME STUDIES BY REFLECTANCE-DIFFERENCE SPECTROSCOPY

D. E. Aspnes, Bellcore, Red Bank, NJ 07701-7040 USA*

ABSTRACT

Reflectance-difference spectroscopy (RDS) is a nondestructive, normal-incidence optical probe that can return direct information about the dielectric properties of of III-V semiconductor crystal surfaces with a sensitivity of about 0.01 monolayer (ML) on time scales of about 0.1s. We have used RDS to study crystal growth by both MBE and OMCVD. For MBE, we obtain directly the anisotropic part of the dielectric response of individual surfaces using a new window, the photoelastic-modulator RD configuration, and a rotating sample. Structure in these data is identified by theoretical calculations. For OMCVD, we establish the kinetics of the (001) GaAs-trimethylgallium(TMG)-arsine system during atmospheric-pressure growth, finding that growth rates are determined by a competition between chemisorption of TMG at individual (001) surface lattice sites at -26 kcal/mole and decomposition of the chemisorbed TMG through a kinetic barrier of 39 kcal/mole. Our model also describes conventional-growth data, indicating that gas-phase chemistry is not as important in OMCVD as commonly believed.

*Work done in collaboration with A. A. Studna, R. Bhat, Y. C. Chang (Univ. of Illinois Urbana-Champaign), E. Colas, L. T. Florez, M. K. Kelly, M. A. Koza, and V. G. Keramidas.

Introduction

A better understanding of crystal growth has become a major goal of materials science as new device designs push present technology to new limits. The need to deal with ever increasing amounts of information places new premiums on device speed and efficiency. Device technology is responding by miniaturizing components, which allows faster and more efficient operation as well as placing more processing power on a single chip, and by developing new device structures, which offer the possibility of operating at still higher speeds.

These trends have influenced crystal growth in several ways. Miniaturization requires more abrupt interfaces and better control of layer thicknesses. Unconventional approaches are being explored to meet these requirements. In molecular beam epitaxy (MBE), growth is interrupted when a sharp interface is needed to allow the ordinarily rough growth surface to smoothen by diffusion. But thickness control is still indirect, being established by maintaining precise oven temperatures previously established by measuring growth rates on preliminary layers by reflection high energy electron diffraction (RHEED). In organometallic chemical vapor deposition (OMCVD), interfaces can be smoothed similarly but the absence of RHEED makes growth-rate determination difficult. Fortunately, the need to decompose non-elemental precursor species such as trimethylgallium and arsine offers the possibility of choosing growth conditions such that decomposition reactions cease when monolayer (ML) coverage is achieved, leading to atomic layer epitaxy (ALE) where layer thicknesses can be determined in principle by multiplying the number of cycles by the thickness of a single ML.

New device designs also incorporate materials according to function, as for example the high-mobility strained-layer pseudomorphic InGaAs base of a GaAs heterojunction bipolar transition. Thus crystal growers must be able essentially to grow anything on anything. Consequently, there is an urgent need to better understand growth processes and to develop methods of controlling crystal growth in real time.

Unfortunately, despite the significant advances of the last 20 years, surface science has very little to offer. Arsenic in MBE chambers coats everything, thereby preventing the use of nearly all surface-analytic tools, while OMCVD is done in sample environments are not only reactive but also at or near atmospheric

pressure. As a result optical probes have come under extensive development as they function equally well in the UHV of an MBE chamber or the atmospheric pressure sample environment of an OMCVD reactor. But optical probes have a low surface sensitivity because optical penetration depths are typically hundreds of times thicker than surface regions. However, three techniques that use symmetry to enhance the weak surface contributions have recently been developed: reflectance-difference spectroscopy (RDS),[1,2] second-harmonic generation (SHG),[3,4] and laser light scattering (LLS).[5,6]

Here, I summarize recent results that we have obtained using RDS to study crystal growth with both MBE and OMCVD. We began[7,8] with MBE growth on (001) GaAs because much is already known about this system and this knowledge can be used to provides insight about the information contained in RD signals. Recent experimental progress[9–11] now allows us to measure the anisotropic part of the surface dielectric response directly, thereby solving the 20-year surface- spectroscopic problem of being able to obtain dielectric-function data about a surface without having to destroy the surface. We have performed theoretical calculations[12] to identify surface dielectric anisotropy (SDA) structure directly and thereby follow the dynamic evolution of different species on the surface as growth conditions are changed.[11] For OMCVD, we have used the time, temperature, partial pressure, and orientational dependences of the evolution of surface species to 0.01 monolayer (ML), 0.1 s precision to establish the kinetics of OMCVD growth[13,14] in the GaAs-trimethylgallium-arsine system.

Experimental

RDS achieves enhanced surface sensitivity by determining the difference between the near-normal-incidence complex reflectances of light linearly polarized along the two principal axes in the plane of the surface. The nearly isotropic bulk contribution cancels in subtraction, leaving that from the lower-symmetry surface. Figure 1 shows our current photoelastic-modulator spectrometer,[8] which has a spectral range of 1.5 to 6.0 eV and is constructed from standard modulation-spectroscopic components: a 75 W Xe short-arc lamp, front-surface spherical and plane mirrors, MgF_2 and quartz Rochon polarizers, a 50 kHz photoelastic modulator, a 0.1 m focusing-grating monochromator with 0.5 mm slits, and an extended S-20 photomultiplier detector. The system functions as an optical bridge, generating signals at 50 and 100 kHz that are proportional to the phase and relative amplitude differences, respectively, between the two complex reflectances. As indicated in Fig. 1, for OMCVD operation the optical beam is simply passed between the turns of the RF heating coil and directly through the well-annealed fused-quartz walls of the reactor. For MBE operation, where ultrahigh vacuum must be maintained for long periods of time, we developed a low-strain fused-quartz window[10] that allows As growth deposits to be removed externally simply by heating.

MBE experiments were performed in a Varian GEN-II system that is equipped with a standard RHEED system and used routinely to produce high quality AlGaAs/GaAs materials and structures. Here, Ga and As are evaporated from effusion ovens and growth is determined by arrival rates and sample temperature. OMCVD experiments were performed with a double-wall atmospheric-pressure OMCVD reactor that is also used routinely to produce high quality AlGaAs/GaAs materials and structures.[15] The atmospheric-pressure (101 kPa) H_2 carrier gas is purified through Pd alloy and flowed laminarly at 19 L/min (average speed 30 cm/s) over the sample surface. Ga is supplied by trimethylgallium (TMG), and As by arsine (AsH_3). In both cases the 5 cm diameter GaAs samples were prepared by standard chemical etching techniques followed by heating to 750 °C in an As-containing environment to remove natural oxides.

Results and discussion: MBE

While early work[7,8] was restricted to measurements of changes of $\Delta R/R$ as sample conditions were changed, where $\Delta R/R$ is the relative difference in reflectances of near-normal-incidence light linearly polarized along the two principal axes of the growth surface, the double modulation provided by the photoelastic

modulator and a rotating sample allows accurate SDA data to be obtained for any given surface.[11] Figure 2 shows several SDA spectra $\Delta(\epsilon d)$ obtained for surfaces of interest to growth on (001) GaAs, including the Ga-stabilized (4× 2) reconstruction and the As-rich intermediate-temperature $(2\times 4)\beta$ and the high-temperature $(2\times 4)\alpha$ phases. Theoretical calculations[11,12] have related the 1.8 and 2.6 eV structures to transitions involving Ga-Ga and As-As dimers, respectively, consistent with their appearance on the associated reconstructions. These data show that the As dimer concentration on the $(2\times 4)\beta$ phase is about twice that on the $(2\times 4)\alpha$ surface, even though both show the same (2× 4) long-range order.

The SDA spectral dependences of Ga-Ga and As-As dimers are such that at 1.8 eV the Ga-Ga and As-As dimer signals reach their peak values in the imaginary and real, respectively, parts of $\Delta(\epsilon d)$, and are nearly zero in the real and imaginary, respectively, parts. This provides an opportunity to follow the relative surface concentrations of the two species during interrupted growth,[11] which appears to be necessary to obtain vertical superlattices.[16,17] Figure 3 shows changes in the real and imaginary parts of $\Delta(\epsilon d)$ when the As fluence is interrupted during otherwise normal growth on a singular (001) GaAs surface and on two vicinal surfaces cut 6° off (001) toward (111)A and (111)B. The substantial differences, including the accommodation of an extra 1/4 ML of Ga-Ga dimers in the singular surface and the appearance of a supersaturation phase transition for the vicinal surface cut toward (111)A shows that steps have a substantial effect on terrace chemistry. These results are also discussed in more detail elsewhere.[11]

Results and discussion: OMCVD

In principle we can perform the same experiments in OMCVD, but in practice refractive-index fluctuations resulting from the cool H_2 carrier gas flowing over the hot sample and susceptor increases the noise of $\Delta\theta$ by an order of magnitude relative to that of $\Delta r/r$, where $\Delta\tilde{r}/\tilde{r} = \Delta r/r + i\Delta\theta$ is the complex-reflectance equivalent to $\Delta R/R$. Consequently, our OMCVD data to date[13,14,18,19] has been directed to understanding the kinetics of the growth process. Typical results[13,14] taken under alternating-flow ALE conditions, where the gas composition in contact with a singular (001) GaAs substrate at 370 °C is changed abruptly at $t = 0$ from H_2 containing 320 Pa AsH_3 to H_2 containing TMG, are shown in Fig. 4. Results for four partial pressures are indicated. The saturation of the reflectance-difference (RD) signal at a common value regardless of TMG partial pressure indicates a surface-site-specific reaction mechanism that is arrested after the active sites have been consumed and ML coverage has been obtained. The 0.01 ML, 0.1 s sensitivity of RD to surface conditions is evident. The partial-pressure dependence immediately indicates that occupancy effects are important, because the rate of generation of the detected byproduct is expected to be proportional to the surface density of active (i.e., occupied) sites. Also surprising is the unconventional time dependence, which is linear to about 80% coverage and exponential beyond (we ignore the initial transient, which is a surface-reordering effect). In a usual surface-poisoning reaction the conversion rate drops by half when half of the sites are consumed, which yields an exponential time dependence. In contrast, Fig. 4 shows that the effective density of active sites is essentially constant until 80% of the surface has reacted.

Using statistics, kinetic theory, detailed balance, and the observed independence of data to small misorientations as described above, we have derived a model that quantitatively describes all these features.[13,14] We identify the reaction sites as surface lattice sites, the reaction species as TMG, and the linear region of the response as being due to steric hindrance, i.e., to the large size of the TMG molecule relative to the spacing of surface lattice sites such that only one in five sites initially can be occupied by a TMG molecule. As the active sites react, new unreacted sites are exposed until the remaining unreacted sites are so far apart that the size of the TMG molecule no longer matters at which point the standard exponential time dependence is observed. The parameters of this model are the attempt frequencies ν_C and ν_D for desorption and decomposition, respectively, of chemisorbed TMG, which we set equal to 400 cm^{-1}; the excluded-volume index m (the number of lattice sites covered by a TMG molecule), which is equal to 5; and the chemisorption enthalpy and decomposition barrier E_C and E_D, which we determine from the 370 ° adsorption isotherm to be -26 and $+39$

kcal/mole, respectively.

In this model the reciprocal of the growth rate (the linearly extrapolated time required to reach 1 ML coverage in Fig. 4) is given by

$$\Delta t = \frac{m}{\nu_D} e^{E_D/kT} [1 + \frac{n_s}{m} \nu_C e^{E_C/kT} \frac{(2\pi M k T)^{1/2}}{P_{TMG}}].$$

This equation describes OMCVD growth as a competition between desorption and decomposition. At low temperatures and/or high TMG pressures where occupancy is near 100%, fractional-occupancy effects represented by the pressure-dependent term are negligible, and an Arrhenius plot yields an apparent activation energy equal to the decomposition barrier E_D = 39 kcal/mole. But at low TMG partial pressures and/or high temperatures where occupancy is low, the fractional-occupancy term dominates and the apparent activation energy is $(E_C + E_D)$ = 13 kcal/mole. At intermediate conditions growth is determined by a blend of the two mechanisms and the apparent activation energy lies between these extremes. In fact, apparent activation energies from 13 to 32 kcal/mole have been reported in the literature.[20-24]

This equation also allows us to compare our model to data in the literature. Figure 5 shows the comparison for our ALE data as well as those of DenBaars et al.,[25] and for several conventional-growth experiments[21,23,25] where temperatures were much higher and TMG and AsH_3 were simultaneously present in the gas stream. The ALE data are in excellent agreement with the predictions, which is not surprising since the model was derived under ALE conditions. But Fig. 5 shows that the model also accurately predicts growth rates and the apparently decreasing activation energy with increasing temperature and decreasing pressure for conventional OMCVD growth as well, at temperatures and conditions where pyrolytic decomposition and gas-phase reactions are expected to occur. As our model is derived entirely from data taken under conditions where these complications cannot occur, we are observing either an unusual coincidence or a fundamental connection among a number of physical parameters, or we must conclude that gas-phase reactions are much less important in OMCVD than previously believed.

Data for the other half of an ALE cycle, the reaction of AsH_3 with the TMG-saturated (001) GaAs surface, are shown in Fig. 6.[18] AsH_3 exposure produces a fast initial transient followed by a slow recovery. The rate of the fast process is independent of AsH_3 partial pressure and sample temperature at least as low as 60 Pa and 340 °C, indicating that the barrier for the reaction between AsH_3 and the TMG-saturated (001) surface is small or nonexistent. We speculate that the slower process is due to the reordering of bonds as the reaction products form the next layer of the crystal. As the time required to reorder the bonds cannot be inferred from the reaction times of the with TMG and AsH_3, the need for real-time control for achieving maximally efficient growth of GaAs by ALE is obvious.

Conclusions

The degrees of freedom provided by time, temperature, cell pressure, precursor species and their partial pressures, deposition rates, surface orientation, and sample history give rise to a wealth of opportunities for further study and ultimately for control of the OMCVD growth process. Further experimental advances will include access to the surface dielectric response with measurements of $\Delta\theta$[9] and the determination of such responses for individual surfaces by double modulation.[11]

References

1. D. E. Aspnes and A. A. Studna, Phys. Rev. Lett. 54, 1956 (1985).

2. D. E. Aspnes, J. Vac. Sci. Technol. **B3**, 1498 (1985).

3. T. F. Heinz, M. J. T. Loy, and S. S. Iyer, Mat. Res. Soc. Symp. Proc. **75**, 697 (1987).

4. S. S. Iyer, T. F. Heinz, and M. M. T. Loy, J. Vac. Sci. Technol. **B5**, 709 (1987).

5. C. Pickering, D. J. Robbins, I. M. Young, J. L. Glasper, M. Johnson, and R. Jones, Mat. Res. Soc. Symp. Proc. **94**, 173 (1987).

6. D. J. Robbins, A. J. Pidduck, A. G. Cullis, N. G. Chew, R. W. Hardeman, D. B. Gasson, C. Pickering, A. C. Daw, M. Johnson, and R. Jones, J. Cryst. Growth **81**, 421 (1987).

7. D. E. Aspnes, J. P. Harbison, A. A. Studna, and L. T. Florez, Phys. Rev. Lett. **59**, 1687 (1987).

8. D. E. Aspnes, J. P. Harbison, A. A. Studna, and L. T. Florez, J. Vac. Sci. Technol. **A6**, 1327 (1988).

9. D. E. Aspnes, A. A. Studna, L. T. Florez, Y. C. Chang, J. P. Harbison, M. K. Kelly, and H. H. Farrell, J. Vac. Sci. Technol. **B7**, 901 (1989).

10. A. A. Studna, D. E. Aspnes, L. T. Florez, J. P. Harbison, and R. Ryan, J. Vac. Sci. Technol. **A7** (in press, Nov/Dec 1989 issue).

11. D. E. Aspnes, Y. C. Chang, A. A. Studna, L. T. Florez, H. H. Farrell, and J. P. Harbison, submitted to Phys. Rev. Lett.

12. Y. C. Chang and D. E. Aspnes, to be submitted to Phys. Rev.

13. D. E. Aspnes, E. Colas, A. A. Studna, R. Bhat, M. A. Koza, and V. G. Keramidas, Phys. Rev. Lett. **61**, 2782 (1988).

14. D. E. Aspnes, R. Bhat, E. Colas, V. G. Keramidas, M. A. Koza, and A. A. Studna, J. Vac. Sci. Technol. **A7**, 711 (1989).

15. R. Bhat, M. A. Koza, C. C. Chang, S. A. Schwartz, and T. D. Harris, J. Cryst. Growth **77**, 7 (1987).

16. T. Fukui and H. Saito, J. Vac. Sci. Technol. **B6**, 1373 (1988).

17. J. M. Gaines, P. M. Petroff, H. Kroemer, R. J. Simes, R. S. Geels, and J. H. English, J. Vac. Sci. Technol **B6**, 1378 (1988).

18. D. E. Aspnes, R. Bhat, E. Colas, M. A. Koza, V. G. Keramidas, and A. A. Studna, Mat. Res. Soc. Symp Proc. **145** (in press).

19. E. Colas, D. E. Aspnes, R. Bhat, A. A. Studna, M. A. Koza, and V. G. Keramidas, J. Cryst. Growth **94** 613 (1989).

20. W. H. Petzke, V. Gottschalch, and E. Butter, Krist. Tech. **9**, 763 (1974).

21. P. W. Lee, T. R. Olmstead, D. R. McKenna, and K. F. Jensen, J. Cryst. Growth **85**, 165 (1987).

22. D. H. Reep and S. K. Ghandi, J. Electrochem. Soc. **130**, 675 (1983).

23. P. Balk, M. Fischer, D. Grundmann, R. Lückerath, H. Lüth, and W. Richter, J. Vac. Sci. Technol. **B5**, 145[illegible] (1987).

24. A. Doi, S. Iwai, T. Meguro, and S. Namba, Jpn. J. Appl. Phys. **27**, 795 (1988).

25. S. P. DenBaars, C. A. Beyler, A. Hariz, and P. D. Dapkus, Appl. Phys. Lett. **51**, 1530 (1987).

Figures

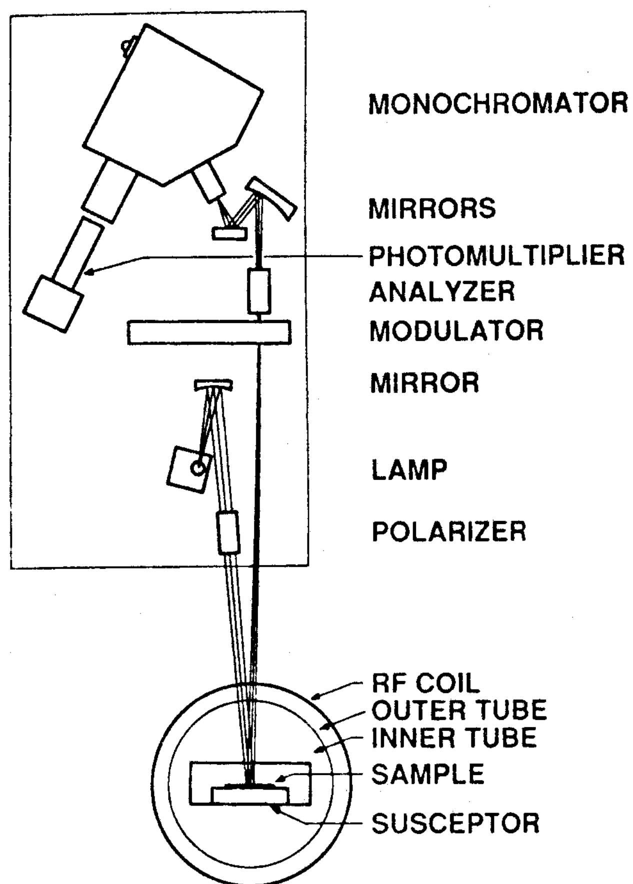

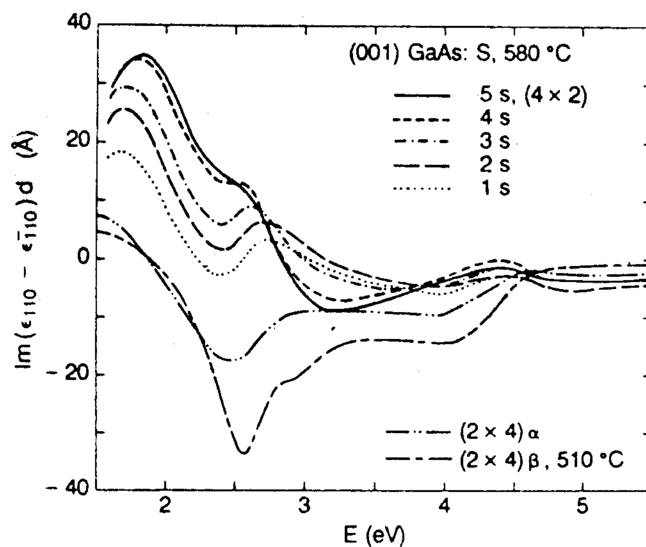

Fig. 1. Schematic diagram of our OMCVD RD spectrometer.

Fig. 2. Surface dielectric anisotropy (SDA) spectra $\Delta(\epsilon_2 d)$ of various reconstructions on (001) GaAs.

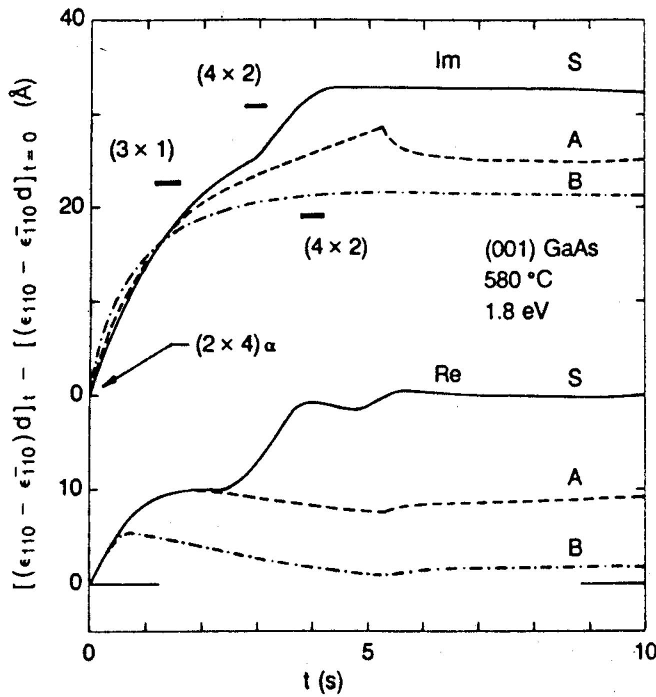

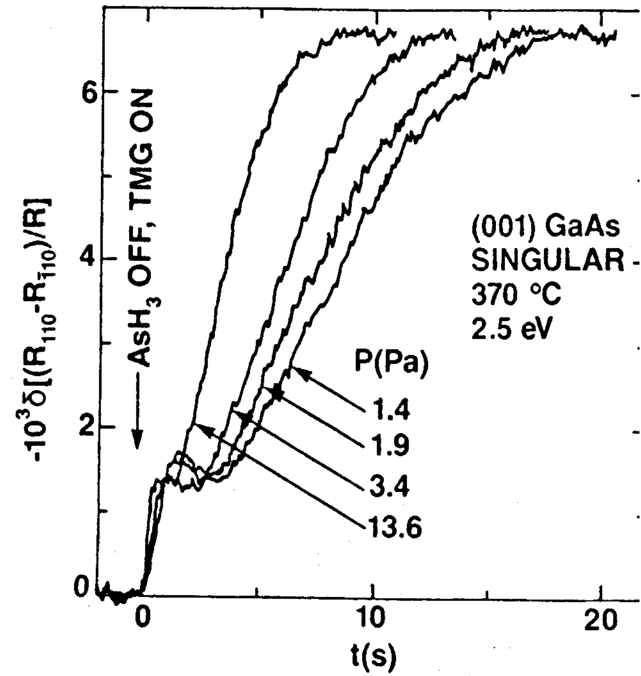

Fig. 3. Changes in the real and imaginary parts of $\Delta(\epsilon d)$ that occur for a singular (001) GaAs surface S an for two vicinal GaAs surfaces A and B cut 6° off (001) toward (111)A and (111)B, respectively. Th onsets of various RHEED reconstruction patterns are also shown.

Fig. 4. Time and pressure dependences of 2.5 eV RD signals for (001) GaAs during atmospheric-pressur ALE growth by OMCVD. Data show results of TMG exposure after AsH_3 saturation.

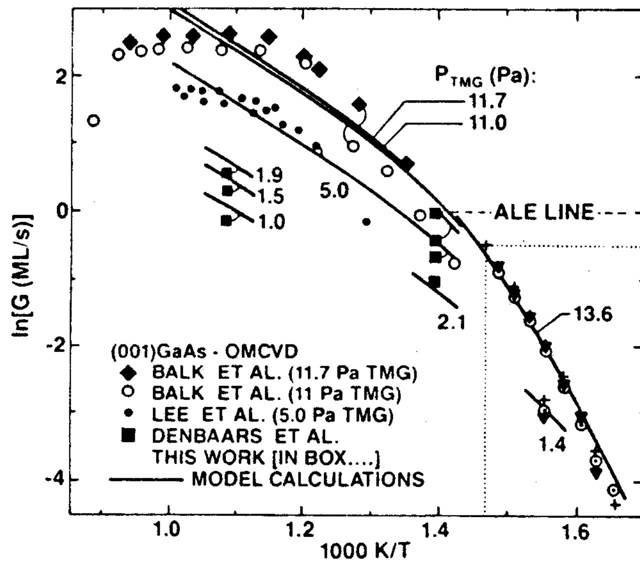

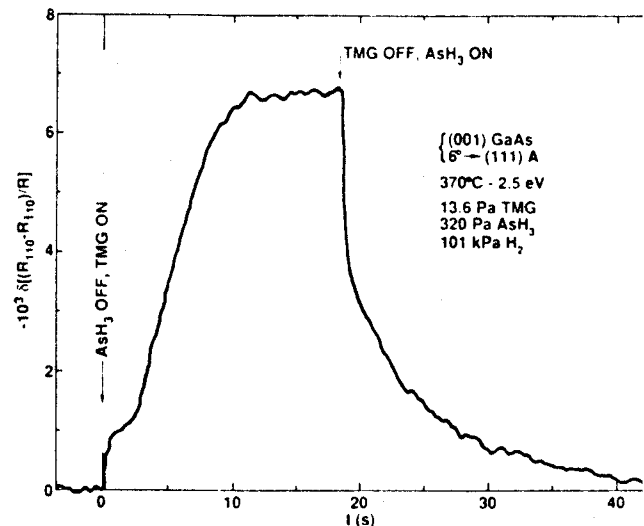

Fig. 5. Arrhenius plots of the growth data obtained here (in box) and from the literature (Lee et al., ref. 21 Balk et al., ref. 23; DenBaars et al., ref. 25) compared to model predictions.

Fig. 6. RD signal at 2.5 eV of a vicinal GaAs sample cut 6° off (001) toward (111)A. A complete AsH_3-TMG AsH_3 atmospheric-pressure ALE growth cycle at 370 ° is shown.